RAA 2020 Vol. **20** No. **11**, 172(8pp) doi: 10.1088/1674-4527/20/11/172

http://www.raa-journal.org *http://iopscience.iop.org/raa*

***R**esearch in*
***A**stronomy and*
***A**strophysics*

The correlations among variability, optical peak time and spectral time lag of long gamma-ray bursts

Bin Liao (廖斌)[1], Yuan-Chuan Zou (邹远川)[1], Fei-Fei Wang (王扉扉)[2], Yu Liu (刘屿)[1] and Wei-Hua Lei (雷卫华)[1]

[1] School of Physics, Huazhong University of Science and Technology, Wuhan 430074, China; *zouyc@hust.edu.cn*
[2] School of Mathematics and Physics, Qingdao University of Science and Technology, Qingdao 266061, China

Received 2019 April 26; accepted 2020 April 25

Abstract Statistical relations are useful tools to comprehend the intrinsic physics processes of gamma-ray bursts (GRBs). In this work we collect spectral lag (τ), variability (V) and optical peak time ($t_{\rm p,o}$). We find that there is a correlation between variabilities and spectral lags, reading as $V = -0.0075(\pm0.0007) \times \log_{10}\tau + 0.0351(\pm0.0024)$. There may also exist a relatively weak positive tendency between GRBs optical band peak times and their spectral time lags. Its Pearson coefficient is 0.398, which indicates a weak linear correlation. If we contain some "negative spectral lag" samples, then the latter relation would be worse due to two outlying points. The $\tau - V$ relation is consistent with previous studies, and the positive trend between τ and $t_{\rm p,o}$ indicates the spectral lag of GRB might be caused by the curvature effect, but this conclusion is not significant.

Key words: gamma-ray burst: general — methods: statistical

1 INTRODUCTION

Gamma-ray bursts (GRBs) are irregular pulses of gamma-ray radiation from the universe (Kumar & Zhang 2015). After decades of research, there still remains many open questions on this spectacular phenomenon. Thanks to the observations made by several γ-ray/X-ray satellites (BeppoSAX, KONUS/Wind, HETE-2, Swift, Integral, AGILE, Fermi) and follow-up observations made by all kinds of observatories (Kumar & Zhang 2015), we are able to obtain various energy bands signals from GRBs. From these observations we may deduce some information on GRBs such as redshift, duration and variability. Correlating these direct or indirect observational parameters may shed light on the intrinsic characters of GRBs. Amati et al. (2002) discovered the positive relation between $E_{\rm p,z}$ and the geometrically-corrected gamma-ray energy $E_{\gamma,\rm iso}$, where $E_{\rm p,z}$ is peak photon energy of prompt spectrum in the source frame of GRBs. Similarly, Wei & Gao (2003); Yonetoku et al. (2004) found the positive correlation between $E_{\rm p,z}$ and $L_{\gamma,\rm p,iso}$, which provided further evidence for Amati relation. Besides, it suggests the overlapping hard-to-soft pulses might cause such intensity-tracking pattern of at least some bursts (Lu et al. 2012). Ghirlanda et al. (2004) found that $E_{\rm p,z}$ was correlated with E_γ (Kumar & Zhang 2015). Besides, relations between three variables were also discovered like Liang-Zhang relation: $E_{\rm p,z} - E_{\gamma,\rm iso} - t_{\rm b,z}$, where $t_{\rm b,z}$ is the afterglow light curve break time in the rest frame of burst (Liang & Zhang 2005).

GRBs spectral lag (τ) is the arrival time difference between high-energy and low-energy photons (Ukwatta et al. 2010). Since the discovery of this phenomenon in 1990s, authors have put forward several models to explain it. It can be explained as the result of spectral evolution of radiation process (e.g., Dermer 1998; Kocevski & Liang 2003; Shao et al. 2017). It can also be explained by geometric effect such as the curvature effect (e.g., Qin et al. 2004; Shen et al. 2005; Lu et al. 2006; Shao et al. 2017). Some other models like quantum theory of gravity, violation of Einstein equivalence principle also predict the time lag when light travels through space. It is also highly possible that spectral lag has more than one origin. Spectral lags can be used to study spectral evolution of GRBs (e.g., Band 1997) and cosmography (e.g., Ellis et al. 2006). Band (1997) studied the time lag of discriminator light curves and found the hard-to-soft evolution of GRBs spectrum. It is also connected with some other parameters of GRBs, such as peak luminosity, which may help us to reveal

the radiation mechanisms and some other characters of GRBs. Norris et al. (2000); Norris (2002); Norris et al. (2005) found an anti-correlation between these two characteristic quantities of GRBs, and Ioka & Nakamura (2001) proposed an off-axis angle model to interpret such relation (Shen et al. 2005).

The variability (V) of GRBs is a quantitative measure of whether its light curve is spiky or smooth (Schaefer 2007). Typically, a larger value of variability means a spikier light curve. To calculate the normalized variance of light curve around a smooth version of this light curve is a reasonable measurement of V (Fenimore & Ramirez-Ruiz 2000), but it involves too many free parameters (Schaefer 2007). Schaefer (2007) improved the definition of variability, and we adopt this definition here. For a background-subtracted light curve (C), they did box smoothing to make a smoothed light curve ($\mathrm{C_{smooth}}$). With these two light curves and uncertainty σ_C, the variability is:

$$V = \left\langle \frac{(C - C_{\mathrm{smooth}})^2 - \sigma_C^2}{C^2_{\mathrm{smooth,max}}} \right\rangle . \quad (1)$$

Despite of different definitions, it still shows a positive correlation with GRB luminosity (Reichart et al. 2001).

After a preliminary correlation analysis, we found there existed possible relation among these quantities, so we did a work on data collection and analysis between spectral lag and variability of prompt phase of GRBs. We also investigated the systematic trend between τ and optical peak time $t_{\mathrm{p,o}}$ of afterglow.

This paper is arranged as follows. In Section 2, we introduce our data collection and selection criteria. In Section 3, we show our analysis method. We present the statistic results and discuss the potential reasons for our results in Section 4.

2 DATA COLLECTION AND CRITERION

We collected three quantities of GRBs: spectral lag (τ), variability (V) and optical band peak time of afterglow phase ($t_{\mathrm{p,o}}$), and discussed two correlations here, namely $\tau - V$ and $\tau - t_{\mathrm{p,o}}$. All data come from papers which have been published. Due to the long distance from GRBs to us, it is quite difficult to know all detailed information. Those GRBs with all parameters data we need are rare. The authors might also calculate spectral lags in GRBs source frame(Bernardini et al. 2015; Wei et al. 2017), but these data are insufficient up to now and so we do not use them here. For the two samples here, we just obtained 49 and 25 GRBs which satisfied the conditions separately. Nearly all of them are long duration GRBs (LGRBs) except GRB 040924A, whose $T90$ is less than 2 s. Therefore, we do not discuss short duration GRBs here. The data are listed in Table 1. We also need to do some transformations because of all kinds problems. See Section 2.1 and Section 2.2 for details.

2.1 $\tau - V$ Relation

We collected 49 GRBs which had both τ and V values. But in different papers, the definitions or calculations of both τ and V may be also different. Spectral time lag (τ) is the time shift between soft and hard light curves of GRBs (Schaefer 2007). Schaefer (2007) took 25–50 keV as soft band and 100–300 keV as hard band, and calculated the time lag between light curves of these two bands. However, Ukwatta et al. (2012) set 100–150 keV and 200–250 keV as soft and hard band separately. This is a common problem (e.g., Ashcraft & Schaefer 2007; Xiao & Schaefer 2011). Considering the narrow energy band range from soft to hard in most papers (in these papers, the energy bands they took are all inside 25–300 keV), we can assume that τ varies with the energy band gap linearly. Then we deduced the average time lag of GRBs (τ_*) using this simple formula:

$$\tau_* = \frac{\tau}{\delta E}, \quad (2)$$

where the energy bands gap δE is defined as the difference between the center of two bands.

Shao et al. (2017) found that the peak arrival time t_{peak} is a function of photon energy E (the mid value of each energy channel), namely:

$$t_{\mathrm{peak}}(E) = t_0 + \tau \times (\frac{E}{1\mathrm{keV}})^{-\beta}, \quad (3)$$

where β is power index. They gave a sample of GRBs and found β varied from 0 and 1. However, this relation only works when each energy band is small enough. Here we take 25-50 keV as soft band and 100-300 keV as hard band. In this situation, a precise model is unnecessary because of the large range of energy band. Figure 2 in Shao et al. (2017) shows that when we choose the energy bands being the edge of the energy range (0-300 keV), we can just use the average spectral time lag, namely τ_* as the calibrated spectral.

Variability has at least three definitions (Schaefer 2007). Meanwhile, data defined in different way are not interconvertible. So we only chose those papers that used the same definition. Here we used the definition of Schaefer (2007). Data of τ and V of GRBs in our sample can be found in Table 1.

2.2 $\tau - t_{\mathrm{p,o}}$ Relation

We collected 25 GRBs which had both τ and $t_{\mathrm{p,o}}$ values. Values of τ were all converted into τ_* as shown in

Table 1 Spectral Lag(τ), Variability(V) and the Optical Peak Time($t_{\rm p,o}$) of GRBs

GRB	Redshift	Normalized Lag ($\times 10^2$ ms MeV^{-1})	Variability ($\times 10^{-3}$)	$t_{\rm p,o}$ (s)	Ref.
910706	···	$3.7^{+3.7}_{-3.7}$	$2.3^{+1.3}_{-1.3}$	···	1,1
911225	···	$3.9^{+5.2}_{-5.2}$	$3.3^{+1.1}_{-1.1}$	···	1,1
920116	···	$3.4^{+2.0}_{-2.0}$	$26.5^{+1.4}_{-1.4}$	···	1,1
920802	···	$2.0^{+1.2}_{-1.2}$	30^{+2}_{-2}	···	1,1
920814B	···	$1.7^{+3.2}_{-3.2}$	13^{+2}_{-2}	···	1,1
921031	···	$0.25^{+0.49}_{-0.49}$	33^{+3}_{-3}	···	1,1
921110	···	$4.4^{+1.4}_{-1.4}$	$19.3^{+0.8}_{-0.8}$	···	1,1
921206	···	$1.85^{+0.25}_{-0.25}$	$13.3^{+0.2}_{-0.2}$	···	1,1
930517	···	$43.2^{+7.8}_{-7.8}$	$20.1^{+1.5}_{-1.5}$	···	1,1
930801	···	56^{+10}_{-10}	5^{+1}_{-1}	···	1,1
940604	···	$6.2^{+2.0}_{-2.0}$	$26.2^{+1.3}_{-1.3}$	···	1,1
941026	···	63^{+12}_{-12}	$9.3^{+0.4}_{-0.4}$	···	1,1
941114	···	$3.4^{+1.6}_{-1.6}$	$38.4^{+1.5}_{-1.5}$	···	1,1
950206	···	$4.9^{+3.0}_{-3.0}$	17^{+1}_{-1}	···	1,1
950223	···	$96.5^{+7.3}_{-7.3}$	$6.8^{+0.2}_{-0.2}$	···	1,1
951007	···	$3.0^{+2.2}_{-2.2}$	$23.9^{+4.4}_{-4.4}$	···	1,1
960418B	···	$5.3^{+2.2}_{-2.2}$	$2.9^{+0.5}_{-0.5}$	···	1,1
960813B	···	$0.12^{+0.25}_{-0.25}$	$12.5^{+0.6}_{-0.6}$	···	1,1
970508A	0.835	31^{+18}_{-18}	$4.7^{+0.9}_{-0.9}$	···	2,3,3
971210	···	$0.12^{+0.98}_{-0.98}$	$24.6^{+0.8}_{-0.8}$	···	1,1
971214B	3.42	$1.8^{+1.8}_{-1.8}$	$15.3^{+0.6}_{-0.6}$	···	2,3,3
980703A	0.966	$24.6^{+6.2}_{-6.2}$	$6.4^{+0.3}_{-0.3}$	···	2,3,4
981130	···	$1.72^{+0.37}_{-0.37}$	$7.7^{+0.4}_{-0.4}$	···	1,1
990123	1.6	$9.8^{+1.8}_{-1.8}$	$17.5^{+0.1}_{-0.1}$	$16.2^{+1.6}_{-1.6}$	2,3,4,5
990216B	···	$5.9^{+6.2}_{-6.2}$	$23^{+0.7}_{-0.7}$	···	1,1
990506A	1.3	$2.5^{+1.2}_{-1.2}$	$13.1^{+0.1}_{-0.1}$	···	2,3,4
990510A	1.619	$1.85^{+0.62}_{-0.62}$	$10^{+0.1}_{-0.1}$	···	2,3,4
000524A	···	$1.97^{+0.61}_{-0.61}$	$22.5^{+0.4}_{-0.4}$	···	1,1
010921A	0.45	55^{+18}_{-18}	$1.4^{+1.5}_{-1.5}$	···	2,3,4
020124	3.2	$4.9^{+3.1}_{-3.1}$	$13.1^{+2.6}_{-2.6}$	···	2,3,4
020813A	1.25	$9.8^{+2.5}_{-2.5}$	$13.1^{+0.3}_{-0.3}$	···	2,3,4
021004A	2.3	37^{+25}_{-25}	$3.8^{+4.9}_{-4.9}$	$30.3^{+8.8}_{-6.7}$	2,3,3,5
030115A	2.5	25^{+12}_{-12}	$6.1^{+4.2}_{-4.2}$	···	6,3,3
030226A	1.986	18^{+18}_{-18}	$5.8^{+4.7}_{-4.7}$	$4340.0^{+3.0}_{-0.7}$	2,3,3,7
030329A	0.169	$8.6^{+2.5}_{-2.5}$	$9.7^{+0.2}_{-0.2}$	···	2,3,4
030429A	2.65	$1.6^{+9.1}_{-9.1}$	$5.5^{+5.7}_{-5.7}$	···	2,8,3
030528A	0.78	769^{+31}_{-31}	$2.2^{+1.9}_{-1.9}$	···	2,3,3
041219A	0.31	$10.9^{+1.5}_{-1.5}$	···	213^{+21}_{-21}	9,10,9
050126	2.29	$133.66^{+0.98}_{-0.98}$	$3.9^{+1.5}_{-1.5}$	···	2,11,3
050318A	1.444	20^{+11}_{-11}	$7.1^{+0.9}_{-0.9}$	···	2,12,3
050401A	2.898	31^{+15}_{-15}	$13.5^{+1.2}_{-1.2}$	···	2,13,3
050505A	4.27	$34.6^{+6.3}_{-6.3}$	$3.5^{+1.9}_{-1.9}$	···	2,11,3
050525A	0.606	27^{+16}_{-16}	$13.5^{+0.3}_{-0.3}$	$41.1^{+10.6}_{-5.6}$	2,14,4,5
050820A	2.615	43^{+18}_{-18}	···	$118.07^{+0.55}_{-0.55}$	2,3,15
050922C	2.198	$13.6^{+6.8}_{-6.8}$	$3.3^{+0.6}_{-0.6}$	···	2,13,4
051111	1.55	33^{+25}_{-25}	$2.4^{+0.7}_{-0.7}$	···	2,13,4
060110	5.0	$46.3^{+6.3}_{-6.3}$	···	$8.3^{+4.2}_{-2.5}$	16,11,5
060124A	2.296	$4.9^{+2.5}_{-2.5}$	14^{+2}_{-2}	···	2,3,3
060210A	3.91	66^{+26}_{-26}	$1.9^{+0.4}_{-0.4}$	$80.0^{+0.2}_{-3.5}$	2,13,4,15
060223A	4.41	$23.4^{+6.2}_{-6.2}$	$7.5^{+3.3}_{-3.3}$	···	17,3,4
060526A	3.22	38^{+15}_{-15}	$11.2^{+3.9}_{-3.9}$	$45.69^{+0.24}_{-0.24}$	2,12,4,15
060605A	3.773	308^{+185}_{-185}	···	$97.00^{+0.21}_{-0.42}$	2,3,15
060607A	3.075	$96.6^{+5.4}_{-5.4}$	$5.9^{+1.4}_{-1.4}$	$52.03^{+0.49}_{-0.49}$	2,11,4,15
060904B	0.703	12^{+44}_{-44}	···	$308.9^{+8.2}_{-1.2}$	18,13,15
060926A	3.2086	$50.2^{+5.4}_{-5.4}$	···	$18.5^{+1.9}_{-1.9}$	2,11,5
061007A	1.262	$5.2^{+2.2}_{-2.2}$	···	$25.6^{+4.2}_{-0.9}$	2,13,15
061121	1.314	$2.2^{+1.0}_{-1.0}$	···	$30.8^{+3.9}_{-0.4}$	2,13,15
061126	1.1588	$4.88^{+0.49}_{-0.49}$	···	$10.7^{+1.4}_{-4.2}$	2,11,5

Table 1 *Continued.*

GRB	Redshift	Normalized Lag ($\times 10^2$ ms MeV^{-1})	Variability ($\times 10^{-3}$)	$t_{\rm p,o}$ (s)	Ref.
071010B	0.95	40^{+16}_{-16}	···	$70.3^{+1.0}_{-1.0}$	2,13,15
080210A	2.641	$25.9^{+8.3}_{-8.3}$	···	$94.92^{+0.28}_{-0.28}$	2,11,15
080319B	0.937	$2.30^{+0.60}_{-0.60}$	···	$14.3^{+4.9}_{-0.5}$	2,13,15
080319C	1.95	$17.4^{+9.1}_{-9.1}$	···	117^{+12}_{-12}	2,13,7
090424A	0.544	$1.4^{+1.4}_{-1.4}$	···	$114.0^{+6.2}_{-1.3}$	2,13,5
091024A	1.092	91^{+60}_{-60}	···	$211.3^{+1.4}_{-1.0}$	2,13,15
100621A	0.542	120^{+31}_{-31}	···	$3443.0^{+0.6}_{-6.2}$	2,13,7
100906A	1.727	$10.5^{+7.9}_{-7.9}$	···	$46.0^{+5.1}_{-0.4}$	2,13,15
110213A	1.46	60^{+75}_{-75}	···	$100.8^{+6.2}_{-0.4}$	2,13,15

The third column lists τ_*, which has been converted into average time lag as mentioned in Sect. 2.1. The fourth column lists peak time of optical band in source frame. Redshift in the first column would be used if we only know the peak time in observed frame. The last column lists the number of references of these parameters, and we simply give the number of data available.
References:(1) Ashcraft & Schaefer (2007); (2) Ruffini et al. (2016); (3) Schaefer (2007); (4) Mosquera Cuesta et al. (2008); (5) Gao et al. (2015); (6) Yonetoku et al. (2004); (7) Ghirlanda et al. (2012); (8) Xiao & Schaefer (2009); (9) Kopač et al. (2013); (10) Foley et al. (2008); (11) Xiao & Schaefer (2011); (12) Li et al. (2012); (13) Ukwatta et al. (2012); (14) Minaev et al. (2014); (15) Beskin et al. (2015); (16) Wei et al. (2014); (17) Racusin et al. (2016); (18) Cano et al. (2017).

Section 2.1. $t_{\rm p,o}$ is the time difference between trigger time and peak flux time in optical band in source frame. Most of these $t_{\rm p,o}$ values came from R-band light curves fitting (Beskin et al. 2015; Gao et al. 2015; Kopač et al. 2013), while some special ones such as GRB080319C was deduced from N-band data (Liang et al. 2010). Considering the large span of $t_{\rm p,o}$ (from 10 to 10^5 s) and relatively small bands difference (hundreds of nanometers), we simply neglect the difference in $t_{\rm p,o}$ from detailed bands like R-band and N-band. Some papers only included data in observers reference, so we need to convert them to the source frame. The data can also be found in Table 1.

3 ANALYSIS METHOD

As mentioned in Section 2, we did some transformations to make sure that all parameters are normalized. After this procedure, we did correlation analysis and tried to find any relation between these parameters. Here, we used five statistical methods to determine whether two parameters are correlated or not. The statistical methods that we used included: Pearson coefficient, Spearman coefficient, Kindall coefficient, cosine similarity, and correlation ratio (Feigelson & Babu 2012). The first four relation coefficients are all quantitative measures of the linearity of two sets of data from different aspects, while the last one judges the nonlinear correlation. From these assessment methods we found that there are potential correlations between these characteristic quantities. Finally, due to the existence of asymmetric error bars in the data of these three quantities, we used Monte Carlo (MC) simulation when we fit these data in linear model.

For a two dimensional data set, with each point being $(x_i{}^{+\sigma_a}_{-\sigma_b}, y_i{}^{+\sigma_c}_{-\sigma_d})$, where $\sigma_a \neq \sigma_b$ and $\sigma_c \neq \sigma_d$, we generate a simulated data set as shown below:

$$x_{i,\rm sim} = \begin{cases} x_i + \xi_{i1} \times \sigma_a, & \xi_{i1} \geq 0, \\ x_i + \xi_{i1} \times \sigma_b, & \xi_{i1} < 0, \end{cases} \tag{4}$$

$$y_{i,\rm sim} = \begin{cases} y_i + \xi_{i2} \times \sigma_c, & \xi_{i2} \geq 0, \\ y_i + \xi_{i2} \times \sigma_d, & \xi_{i2} < 0, \end{cases} \tag{5}$$

where ξ_{i1} and ξ_{i2} are both random numbers that follow standard normal distribution. For each simulated data set we can get a set of fitting parameters and statistical coefficients. Here we made 10^5 times simulations and obtained the distributions of these parameters. From the distributions we can deduce the center values and uncertainties of fitting parameters and statistical coefficients, including slope, intercept, Pearson coefficient and so on. Figure 1 includes the distribution of slope and intercept of $\tau_* - V$ fitting, and Figure 2 shows the result of $\tau_* - t_{\rm p,o}$. They all follow the Gauss distribution, and so we simply take the central value and standard deviation as our fitting central value and 1σ error bar. The other parameters, like Pearson coefficient, are all deduced from this method.

4 RESULTS AND DISCUSSION

4.1 τ_*-V

Figure 3 shows the correlation between spectral lags and variabilities of GRBs in our sample. There are 49 samples in this panel. The red points mean their 1σ confidence intervals contain zero in normal coordinate. When we did the transformation from normal coordinate to logarithmic coordinate, the difficulty arose. Similar with some previous works (Ukwatta et al. 2010, 2012; Bernardini et al. 2015),

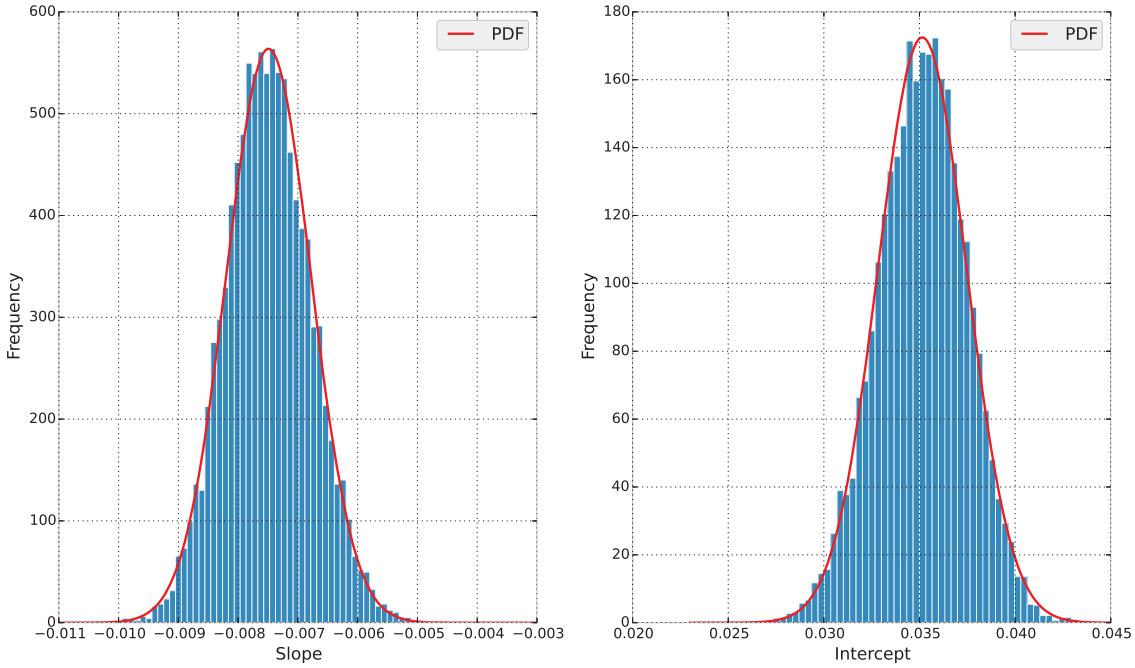

Fig. 1 10^5 MC simulation realizations for $\tau_* - V$ fitting. The left panel shows the probability density function (PDF) of the slope while the right panel shows the intercept.

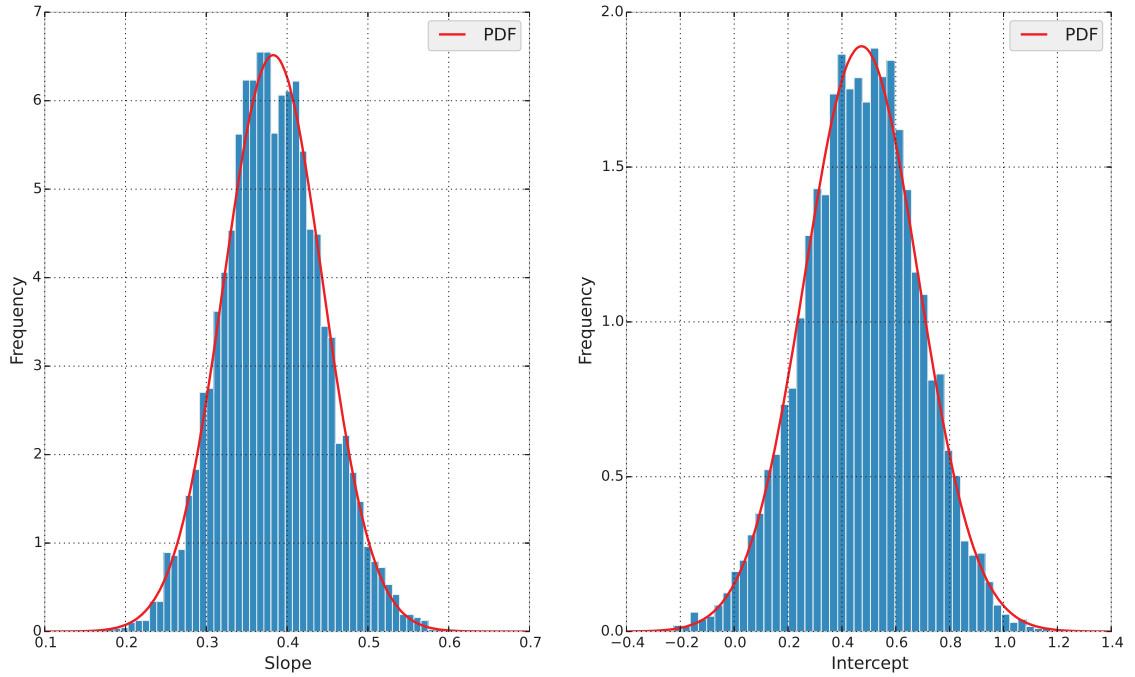

Fig. 2 The same as Fig. 1, but corresponds to $\tau_* - t_{\rm p,o}$ fitting.

we did not consider such samples firstly (10; 20.4% of the total samples). All the central values of lags in our samples are positive. The blue points are samples we fit with linear model involving MC method, and the black line shows the fitting result. The black line is the best fit to the data using MC simulation. From the figure, we can deduce that there is an obvious negative trend between these two quantities. Pearson coefficient of blue points is -0.564, meaning a relatively good linearity, while the high value of correlation ratio shows a nonlinear model is also a good choice. Detailed fitting parameters and correlation coefficients are displayed in Table 2.

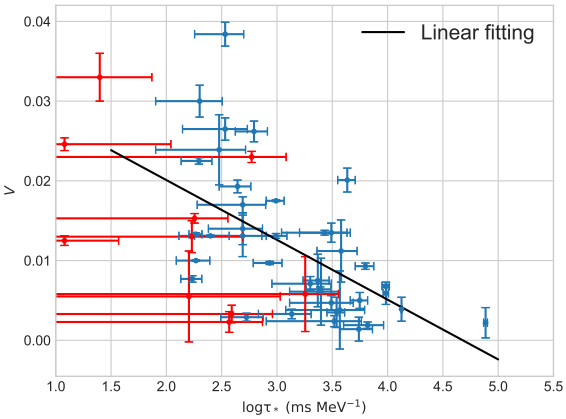

Fig. 3 Variability (V) as a function of spectral lag (τ_*). The red points represent those 1σ error including zero samples, and the blue points are samples whose lags are well above zero. The black solid line is the best linear fit using MC simulation, and its expression is $V = -0.0075(\pm0.0007) \times \log_{10}\tau + 0.0351(\pm0.0024)$.

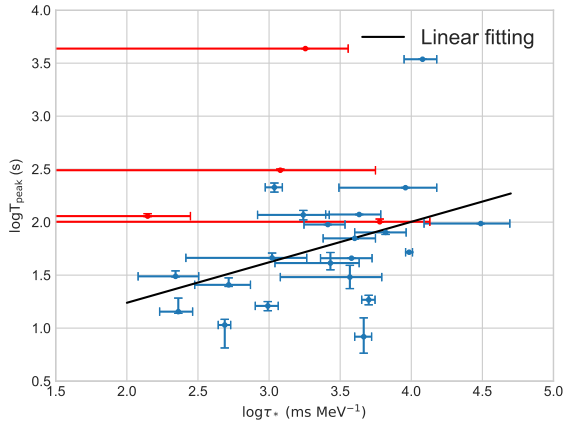

Fig. 4 Optical peak times ($t_{\rm p,o}$) versus the spectral time lag (τ_*). The data are the same as those in Fig. 3. The black solid line is the best linear fitting line using MC simulation, and its expression is $\log_{10} t_{\rm p,o} = 0.382(\pm0.062) \times \log_{10}\tau + 0.475(\pm0.214)$.

There usually is a time difference between the arrival time of soft photons and hard photons in GRBs. However, the reasons for this spectral lag are still controversial. As we have discussed in introduction, the spectral lags may have more than one origin. For different origins, spectral lag may show diverse properties. From our results we may give some constraints on these models.

Variability represents the complexity of GRB light curves (Kumar & Zhang 2015). Its definition varies among authors. In principle, it should be closely correlated with the prompt emission of GRBs. Fernimore and Ramirez-Ruiz and Reichart et al. (2001) proposed correlation between GRB luminosity and variability (Kumar & Zhang 2015). Despite different definitions, it was found that there existed a positive correlation between V and peak luminosity: $L_{\gamma,\rm p,iso} \propto V^m$, where the index m ranges from 3.3 (Reichart et al. 2001) to 1.1 (Guidorzi et al. 2005). This relation hints at the potential correlations between V and some other characters of prompt emission like τ_*, the spectral lag. Figure 3 shows an obvious anti-correlation between these two parameters. Here we cannot explain the intrinsic reason for this picture, but it helps to test some other discovered physics. Norris et al. (2000) found an anti-correlation between spectral lag (τ in the observer frame) and peak luminosity ($L_{\gamma,\rm p,iso}$), reads

$$L_{53} \approx 1.3 \times (\tau/0.01\,{\rm s})^{-1.14}, \quad (6)$$

where L_{53} is the luminosity in unit of $10^{53}{\rm erg\,s^{-1}}$. Some others considered lags in the rest frame and obtained similar results. From these two relations ($L-V$ and $L-\tau$) above, we may easily deduce a simple negative correlation between τ_* and V. On this point, Figure 3 displays a consistent result. Note that we use the normalized τ_* instead of the direct spectral lag of two light curves in different energy bands.

Table 2 Correlation Coefficients between τ_* and V and Fitting Parameters

Correlation Coefficients		
coefficient type	value	p-value
Pearson	-0.564 ± 0.049	0.00019
Spearman	-0.586 ± 0.053	0.00009
Kendall	-0.411 ± 0.043	0.00023
correlation ratio	0.957 ± 0.004	
cosine similarity	0.708 ± 0.017	
Linear fitting using MC		
$V = -0.0075(\pm0.0007) \times \log_{10}\tau_* + 0.0351(\pm0.0024)$		

4.2 τ_*-$t_{\rm p,o}$

For the same reason mentioned in Section 4.1, we do not consider four points whose central values are positive but 1σ error bar containing zero. The left samples contain 22 data points, which are shown in Figure 4. The black line shows the fitting result as well. Pearson coefficient of these samples is 0.398, meaning a relatively weak linearity, but the positive correlation between τ_* and $t_{\rm p,o}$ is obvious. Detailed results are displayed in Table 3.

In Figure 4, we may find a clear positive trends between τ_* and $t_{\rm p,o}$. This result is interesting for their different emission region (τ_* is the spectral time lag of gamma-ray prompt emission while $t_{\rm p,o}$ belongs to afterglow). Here we can interpret the result using the

curvature model of time lag. Sari & Piran (1997) described the angular spreading model. Considering an advancing spherical shock whose Lorentz factor is Γ and radius is R. Because of radiation beaming, we can only see photons up to solid angle of Γ^{-1}. Two photons are emitted simultaneously, but one is from the line of sight while the other is from an angle of Γ^{-1} away. The arrival time delay due to this factor is

$$T_{\rm angular} \approx R/2\Gamma^2 c, \tag{7}$$

where the approximation $\cos\theta \approx 1-\theta^2/2$ has been used. This timescale is called angular spreading timescale.

In the curvature model, the spectral lag should scale with this angular spreading timescale (Sonbas et al. 2015). That means a direct correlation between τ_* and Γ. Several papers gave different results. But they all gave a negative correlation between τ_* and Γ, i.e.

$$\tau_* \propto \Gamma^{-\alpha}, \tag{8}$$

where α should be a positive number (Qin et al. 2004; Shen et al. 2005; Lu et al. 2006). Shen et al. (2005) showed α was around 1 while Lu et al. (2006) got the result that it was at least 2 and varied with energy band.

Meanwhile, $t_{\rm p,o}$ is closely correlated with the deceleration time. In the constant ISM,

$$t_{\rm p,o} \propto \Gamma^{-\beta}, \tag{9}$$

where $\beta = 8/3$ for adiabatic blast wave and $\beta = 7/3$ for the radiative case (Sonbas et al. 2015). From the expression of τ_* and $t_{\rm p,o}$ on Γ, we may easily deduce the following two relations:

$$\frac{t_{\rm p,o}}{\tau_*} \propto \Gamma^{\alpha-\beta}, \tag{10}$$

$$\mathrm{S}_{\log t_{\rm p,o},\log\tau_*} = \frac{\beta}{\alpha}, \tag{11}$$

where "S" denotes the slope between $\log t_{\rm p,o}$ and $\log\tau_*$ like Figure 4. From Equation (10) we know these two quantities are positively correlated, and in Equation (11) we may get a rough result in that if we assumed a linear relationship between them, then the slope of $\log t_{\rm p,o}$ and $\log\Gamma$ would be around β/α. Its value should vary around 1 to 3 for different models. For example, Shen et al. (2005) calculated a series of spectral lags using curvature model from a set of relatively large range parameters. They assumed the intrinsic spectral lag to be less than 1 s, and the Lorentz factor of emission area above 50, which might ignore some other possibility. Their result shows most spectral lags are shorter than 0.1 s, which is obviously different from the real situation. The curvature model might show quite different result for some extreme values like small Lorentz factor because beaming effect become invalid and spreading time would be wrong with this situation. This might be why the predicted value shows at most seven times larger than our fitting result. This relation also suggests a direct link between the prompt emission and the afterglow emission through Lorentz factor of emission region.

Table 3 Correlation Coefficients between τ_* and $t_{\rm p,o}$ and Fitting Parameters

Correlation Coefficients		
coefficient type	value	p-value
Pearson	0.398 ± 0.051	0.073
Spearman	0.372 ± 0.075	0.096
Kendall	0.255 ± 0.058	0.103
correlation ratio	0.812 ± 0.016	
cosine similarity	0.959 ± 0.003	
Linear fitting using MC		
$\log_{10} t_{\rm p,o} = 0.382(\pm0.062) \times \log_{10}\tau_* + 0.475(\pm0.214)$		

5 CONCLUSION AND DISCUSSION

In this work we collected data of three parameters of GRBs: spectral lag, variability and optical peak time and did correlation analysis. We found that there existed a negative correlation between variabilities and spectral lags. This shows an opposite trend between optical peak times and lags. The former result $V = -0.0075(\pm0.0007) \times \log_{10}\tau_* + 0.0351(\pm0.0024)$ helps us to verify some relations which have been found before (Norris et al. 2000; Reichart et al. 2001). The latter relation $\log_{10} t_{\rm p,o} = 0.382(\pm0.062) \times \log_{10}\tau_* + 0.475(\pm0.214)$ might be caused by the curvature model. The $t_{\rm p,o} - \tau_*$ relation is also a bridge and tie to link prompt emission stage and afterglow stage of GRBs, which is intriguing.

Here, we have not discussed those negative central spectral lag situations due to limited samples. This reflects the relative rarity of negative spectral lag to some degree. The incomplete samples may also introduce bias. The clustering of spectral lag in Figure 3 is also noteworthy. The samples are divided by the boundary $\tau_* = 10^3$ s. Such a character may indicate a different origin. The negative 1σ error bar for some points is also a confusing problem. Because it has various potential sources, spectral lag may exhibit different evolution with frequency (Wei et al. 2017). The negative value of lag may also indicate an entirely different physics origin, especially for the emission mechanism and radiation region.

In our calculation above, we did not consider those data which could fall below zero because of the difficulty in coordinate transformation, but it could introduce a bias. Here we do an analysis that is not rigorous. First, the

general trend of these two pairs of quantities should not change no matter whether we take these red points in Figure 3 and Figure 4. Second, if we just consider the center values regardless of error bars, we calculate the Pearson coefficients and corresponding p-value as well. The Pearson coefficient and p-value of $\tau_* - V$ case are –0.55 and 4.3×10^{-5} respectively, while for $\tau_* - t_{\rm p,o}$ case they are 0.27 and 0.18, respectively. From these calculations we may get a qualitative conclusion that the negative linear correlation between τ_* and V is strong enough, but the linear correlation between another pair of quantities, τ_* and $t_{\rm p,o}$, maybe only suitable for a small part of GRBs, because if we did not consider the two obvious outlying points, the correlation would be relatively credible.

Acknowledgements This work is supported by the National Basic Research Program ('973' Program) of China (Grant No. 2014CB845800) and by the National Natural Science Foundation of China (Grant No. 11773010). This research is also supported in part by Perimeter Institute for Theoretical Physics. Research at Perimeter Institute is supported by the Government of Canada through the Department of Innovation, Science and Economic Development Canada and by the Province of Ontario through the Ministry of Economic Development, Job Creation and Trade.

References

Amati, L., Frontera, F., Tavani, M., et al. 2002, A&A, 390, 81
Ashcraft, T., & Schaefer, B. E. 2007, ApJ, 671, 1896
Band, D. L. 1997, ApJ, 486, 928
Bernardini, M. G., Ghirlanda, G., Campana, S., et al. 2015, MNRAS, 446, 1129
Beskin, G. M., Oganesyan, G., Greco, G., & Karpov, S. 2015, Astrophysical Bulletin, 70, 400
Cano, Z., Wang, S.-Q., Dai, Z.-G., & Wu, X.-F. 2017, Advances in Astronomy, 2017, 8929054
Dermer, C. D. 1998, ApJL, 501, L157
Ellis, J., Mavromatos, N. E., Nanopoulos, D. V., et al. 2006, Astroparticle Physics, 25, 402
Feigelson, E. D., & Babu, G. J. 2012, Modern Statistical Methods for Astronomy (Cambridge: Cambridge Univ. Press)
Fenimore, E. E., & Ramirez-Ruiz, E. 2000, arXiv e-prints, astro-ph/0004176
Foley, S., McGlynn, S., Hanlon, L., et al. 2008, A&A, 484, 143
Gao, H., Wang, X.-G., Mészáros, P., & Zhang, B. 2015, ApJ, 810, 160
Ghirlanda, G., Ghisellini, G., & Lazzati, D. 2004, ApJ, 616, 331
Ghirlanda, G., Nava, L., Ghisellini, G., et al. 2012, MNRAS, 420, 483
Guidorzi, C., Frontera, F., Montanari, E., et al. 2005, MNRAS, 363, 315
Ioka, K., & Nakamura, T. 2001, ApJL, 554, L163
Kocevski, D., & Liang, E. 2003, ApJ, 594, 385
Kopač, D., Kobayashi, S., Gomboc, A., et al. 2013, ApJ, 772, 73
Kumar, P., & Zhang, B. 2015, Phys. Rep., 561, 1
Li, Z., Chen, L., & Wang, D. 2012, PASP, 124, 297
Liang, E.-W., Yi, S.-X., Zhang, J., et al. 2010, ApJ, 725, 2209
Liang, E., & Zhang, B. 2005, ApJ, 633, 611
Lu, R. J., Qin, Y. P., Zhang, Z. B., & Yi, T. F. 2006, MNRAS, 367, 275
Lu, R.-J., Wei, J.-J., Liang, E.-W., et al. 2012, ApJ, 756, 112
Minaev, P. Y., Pozanenko, A. S., Molkov, S. V., & Grebenev, S. A. 2014, Astronomy Letters, 40, 235
Mosquera Cuesta, H. J., Dumet M, H., & Furlanetto, C. 2008, J. Cosmol. Astropart. Phys., 2008, 004
Norris, J. P. 2002, ApJ, 579, 386
Norris, J. P., Bonnell, J. T., Kazanas, D., et al. 2005, ApJ, 627, 324
Norris, J. P., Marani, G. F., & Bonnell, J. T. 2000, ApJ, 534, 248
Qin, Y.-P., Zhang, Z.-B., Zhang, F.-W., & Cui, X.-H. 2004, ApJ, 617, 439
Racusin, J. L., Oates, S. R., de Pasquale, M., & Kocevski, D. 2016, ApJ, 826, 45
Reichart, D. E., Lamb, D. Q., Fenimore, E. E., et al. 2001, ApJ, 552, 57
Ruffini, R., Rueda, J. A., Muccino, M., et al. 2016, ApJ, 832, 136
Sari, R., & Piran, T. 1997, ApJ, 485, 270
Schaefer, B. E. 2007, ApJ, 660, 16
Shao, L., Zhang, B.-B., Wang, F.-R., et al. 2017, ApJ, 844, 126
Shen, R.-F., Song, L.-M., & Li, Z. 2005, MNRAS, 362, 59
Sonbas, E., MacLachlan, G. A., Dhuga, K. S., et al. 2015, ApJ, 805, 86
Ukwatta, T. N., Stamatikos, M., Dhuga, K. S., et al. 2010, ApJ, 711, 1073
Ukwatta, T. N., Dhuga, K. S., Stamatikos, M., et al. 2012, MNRAS, 419, 614
Wei, D. M., & Gao, W. H. 2003, MNRAS, 345, 743
Wei, J.-J., Wu, X.-F., Melia, F., Wei, D.-M., & Feng, L.-L. 2014, MNRAS, 439, 3329
Wei, J.-J., Zhang, B.-B., Shao, L., Wu, X.-F., & Mészáros, P. 2017, ApJL, 834, L13
Xiao, L., & Schaefer, B. E. 2009, ApJ, 707, 387
Xiao, L., & Schaefer, B. E. 2011, ApJ, 731, 103
Yonetoku, D., Murakami, T., Nakamura, T., et al. 2004, ApJ, 609, 935